mathematics

MDPI

Article

Computer Analysis of Human Belligerency

José A. Tenreiro Machado [1,†], António M. Lopes [2,*,†] and Maria Eugénia Mata [3,†]

1 Department of Electrical Engineering, Institute of Engineering, Polytechnic of Porto, Rua Dr. António Bernardino de Almeida, 431, 4249-015 Porto, Portugal; jtm@isep.ipp.pt
2 LAETA/INEGI, Faculty of Engineering, University of Porto, Rua Dr. Roberto Frias, 4200-465 Porto, Portugal
3 Nova SBE, Nova School of Business and Economics (Faculdade de Economia da Universidade Nova de Lisboa), Rua da Holanda, 1, 2775-405 Carcavelos, Portugal; memata@fe.unl.pt
* Correspondence: aml@fe.up.pt
† These authors contributed equally to this work.

Received: 13 June 2020; Accepted: 20 July 2020; Published: 22 July 2020

Abstract: War is a cause of gains and losses. Economic historians have long stressed the extreme importance of considering the economic potential of society for belligerency, the role of management of chaos to bear the costs of battle and casualties, and ingenious and improvisation methodologies for emergency management. However, global and inter-temporal studies on warring are missing. The adoption of computational tools for data processing is a key modeling option with present day resources. In this paper, hierarchical clustering techniques and multidimensional scaling are used as efficient instruments for visualizing and describing military conflicts by electing different metrics to assess their characterizing features: time, time span, number of belligerents, and number of casualties. Moreover, entropy is adopted for measuring war complexity over time. Although wars have been an important topic of analysis in all ages, they have been ignored as a subject of nonlinear dynamics and complex system analysis. This paper seeks to fill these gaps in the literature by proposing a quantitative perspective based on algorithmic strategies. We verify the growing number of events and an explosion in their characteristics. The results have similarities to those exhibited by systems with increasing volatility, or evolving toward chaotic-like behavior. We can question also whether such dynamics follow the second law of thermodynamics since the adopted techniques reflect a system expanding the entropy.

Keywords: data visualization; multidimensional scaling; hierarchical clustering; entropy; complex systems

1. Introduction

Wars have played a major role in human history, because they have long accounted for violence. According to Blum [1], we presently live in a paradox of power, because on the one hand our means and methods of war have become both more devastating (potentially), and on the other hand less devastating (in practice).

Campbell [2] asks what conception of war to adopt. Williams et al. [3] (p. 85) recall that Cicero defined war as contending by force, and Machiavelli [4] installed Machiavellian philosophy in saying that "rulers should be good if they can, but be willing to practice evil if necessary" in order to reach their goals. In the same way, Grotius [5] (p. 18) wrote that "war is the state of contending parties, considered as such," while for Hobbes [6] war was a state of affairs. Regretting wars, Mannies and Laursen [7] prefer to say that war is a violent political disease.

How can one account for wars? The mathematical analysis of war has relied on developing and interpreting the statistical distributions of casualties [8,9]. Such distributions reveal fat-tails, meaning that the size of an event is inversely proportional to its frequency. Such patterns can be used to predict the size distribution of future wars, with implications in sociological and general policy [10].

The fat-tail distributions are consistent with self-similarity, scale-invariance, and self-organized criticallity mechanisms, as reported in various studies [11–14].

This paper uses a framed database to record wars, military struggles, and armed conflicts over time. Data are interpreted and patterns unveiled according to different distances between high-dimensional data, namely, time and space proximity (by the date and parts involved); and human sacrifice or human capital loss (by the number of casualties) using the hierarchical clustering (HC) and multidimensional scaling (MDS) computational visualization techniques. Moreover, entropy is adopted as a measure of characterizing war data, when regarded as the output of a complex system. On the difficulty of such an exercise, which checks the historical decisions of commander-in-chiefs for fighting with sets of historical conditions and military weaponry, Milward [15] says, quoting Carl von Clausewitz (1833), that "Bonaparte was quite right when he said that many of the decisions which confront a commander-in-chief would constitute problems in mathematical calculus not unworthy of a Newton and a Euler."

The synergies of adopting data analysis and computational strategies reveal the key importance of this manifestation of the intrinsic behavior of the human species. The historical records provide assertive quantitative information and the results of the analysis give a new perspective towards the future development of modeling strategies. Having these ideas in mind, the modeling follows present day data processing techniques, using computational resources both for data analysis and for the visualization of the results. The HC and MDS are useful algorithms for time series analysis, embedding several characteristics such as time, time span, number of belligerents, and number of casualties. The results reveal that the treatment of real-world data may unveil details not qualitatively known with standard approaches. On the other hand, the entropy analysis of the war casualties, interpreted as the output of a complex system, reveals the human-belligerency trend towards "chaotic-like" behavior over time. This evolution toward a state of higher confusion reveals increasing an entropy, somehow compatible with systems following the second law of thermodynamics.

The paper has the following organization. Section 2 presents the mathematical fundamentals, namely, the HC and MDS techniques, the distances for assessing historical data records, and the concepts of entropy and spectral entropy. Section 3 describes the dataset used and develops the computational modeling approach using the HC and MDS. Section 4 interprets the results from a sociological perspective. Section 5 analyses the data by means of entropy generated by a complex system. Finally, section 6 outlines the main conclusions.

2. Fundamental Concepts and Tools

2.1. Distance Indices

A function is considered a distance, $d(\mathbf{v}_i, \mathbf{v}_j)$, between $\mathbf{v}_i$ and $\mathbf{v}_j$, if it obeys the following axioms: (i) non-negativity, (ii) identity of indiscernibles, (iii) symmetry, and (iv) triangle inequality [16].

In the sequel, nine distances are considered for comparing objects, namely, the $\{$Arccosine, Canberra, Dice, Divergence, Euclidean, Jaccard, Lorentzian, Manhattan, and Sørenson$\} = \{d_1, \ldots, d_9\}$ distances. Accordingly, given the points $\mathbf{v}_i = (v_{i1}, \cdots, v_{iP})$ and $\mathbf{v}_j = (v_{j1}, \cdots, v_{jP})$ in a P dimensional space, the distances between $\mathbf{v}_i$ and $\mathbf{v}_j$ are given by [16]:

$$d_1(\mathbf{v}_i, \mathbf{v}_j) = \arccos\left(\frac{\sum_{k=1}^{P} v_{ik} \cdot v_{jk}}{\sqrt{\sum_{k=1}^{P} v_{ik}^2}\sqrt{\sum_{k=1}^{P} v_{jk}^2}}\right), \tag{1}$$

$$d_2(\mathbf{v}_i, \mathbf{v}_j) = \sum_{k=1}^{P} \frac{|v_{ik} - v_{jk}|}{|v_{ik}| + |v_{jk}|}, \tag{2}$$

$$d_3(\mathbf{v}_i, \mathbf{v}_j) = \frac{2\sum_{k=1}^{P} v_{ik} \cdot v_{jk}}{\sum_{k=1}^{P} v_{ik}^2 + \sum_{k=1}^{P} v_{jk}^2}, \tag{3}$$

$$d_4(\mathbf{v}_i, \mathbf{v}_j) = 2\sum_{k=1}^{P} \frac{(v_{ik} - v_{jk})^2}{(v_{ik} + v_{jk})^2}, \tag{4}$$

$$d_5(\mathbf{v}_i, \mathbf{v}_j) = \sqrt{\sum_{k=1}^{P} (v_{ik} - v_{jk})^2}, \tag{5}$$

$$d_6(\mathbf{v}_i, \mathbf{v}_j) = \frac{\sum_{k=1}^{P} (v_{ik} - v_{jk})^2}{\sum_{k=1}^{P} v_{ik}^2 + \sum_{k=1}^{P} v_{jk}^2 - \sum_{k=1}^{P} v_{ik} v_{jk}}, \tag{6}$$

$$d_7(\mathbf{v}_i, \mathbf{v}_j) = \sum_{k=1}^{P} \ln\left(1 + |v_{ik} - v_{jk}|\right). \tag{7}$$

$$d_8(\mathbf{v}_i, \mathbf{v}_j) = \sum_{k=1}^{P} |v_{ik} - v_{jk}|, \tag{8}$$

$$d_9(\mathbf{v}_i, \mathbf{v}_j) = \frac{\sum_{k=1}^{P} |v_{ik} - v_{jk}|}{\sum_{k=1}^{P} (v_{ik} + v_{jk})}, \tag{9}$$

The Arccosine distance is important when comparing objects described by vectors with different magnitudes. The Canberra is a metric well-suited for quantifying data scattered around an origin and is very sensitive for values close to zero. The Dice, like the Arccosine and the Jaccard, is an angularly-based measure closely related to the Euclidean distance, which is the shortest distance between two points. In particular, the Jaccard has several practical applications, namely, in information retrieval, data mining, and machine learning. The Divergence measures the "distance" between two probability distributions on a statistical manifold. The Lorentzian is the natural logarithm of an absolute difference between objects. The Manhattan distance is a rectilinear distance or taxicab norm. The Sørenson distance is close to the Canberra.

2.2. Hierarchical Clustering

Let us consider a set of N objects, $\mathbf{v}_i$, $i = 1, \ldots, N$, in a P dimensional real-valued space. The HC is a technique that visualizes groups of similar objects and involves three steps [17]. The first consists of defining a measure of the distance $d(\mathbf{v}_i, \mathbf{v}_j)$, $i, j = 1, \ldots, N$, between the objects i and j. The second step regards the comparison of all objects and the construction of a matrix of distances, $\mathbf{D} = [d(\mathbf{v}_i, \mathbf{v}_j)]$, of dimensions $N \times N$. For classical distances, $d(\mathbf{v}_i, \mathbf{v}_j) = d(\mathbf{v}_j, \mathbf{v}_i)$ the matrix $\mathbf{D}$ is symmetric, with zeros in the main diagonal. In the final step the HC algorithm produces a structure of clusters that is represented by some graphical portrait, such as a hierarchical tree or a dendrogram. We can adopt two main techniques: (i) the agglomerative and (ii) the divisive iterative schemes. For the agglomerative, each object starts in its own cluster. Then, the successive iterations join the most similar clusters until reaching one single cluster. For the divisive scheme, all objects start in a single cluster. Then, the iterations remove the "outsiders" from the least cohesive cluster, until each object has a separate cluster. The HC requires the definition of a linkage criterion, consisting of some distances, for quantifying the dissimilarity between clusters. The distance $d(\mathbf{v}_R, \mathbf{v}_S)$ between a pair of objects $\mathbf{v}_R \in R$ and $\mathbf{v}_S \in S$, in the clusters R and S, respectively, can be determined by means of a number of alternative metrics, such as the average-linkage [18]:

$$d_{av}(R, S) = \frac{1}{\|R\| \, \|S\|} \sum_{\mathbf{v}_R \in R, \mathbf{v}_S \in S} d(\mathbf{v}_R, \mathbf{v}_S). \tag{10}$$

For assessing the quality of the clustering, we can adopt the cophenetic coefficient *cc* [19]. Let us assume that the objects $\mathbf{v}_i$ and $\mathbf{v}_j$ are described by the HC representations $\mathbf{t}_i$ and $\mathbf{t}_j$, respectively; then the index *cc* is given by:

$$cc = \frac{\sum\limits_{i<j} \left[d(\mathbf{v}_i, \mathbf{v}_j) - \bar{v}\right] \left[d(\mathbf{t}_i, \mathbf{t}_j) - \bar{t}\right]}{\sqrt{\left[\sum\limits_{i<j} \left[d(\mathbf{v}_i, \mathbf{v}_j) - \bar{v}\right]^2\right] \left[\sum\limits_{i<j} \left[d(\mathbf{t}_i, \mathbf{t}_j) - \bar{t}\right]^2\right]}}, \tag{11}$$

where $\bar{v} = \text{av}\left(d(\mathbf{v}_i, \mathbf{v}_j)\right)$ and $\bar{t} = \text{av}\left(d(\mathbf{t}_i, \mathbf{t}_j)\right)$, with $\text{av}(\cdot)$ denoting average, and $d(\mathbf{t}_i, \mathbf{t}_j)$ is the cophenetic distance between the HC objects $\mathbf{t}_i$ and $\mathbf{t}_j$. We have $0 \leq cc \leq 1$ and the limits correspond to bad and good clustering of the original data. Additionally, the Shepard chart can be used to compare the original and the cophenetic distances, so that the closer the points to the 45 degree line, the better the result. The graphical portrait consists of a dendogram or a tree, and the objects are the "leafs".

2.3. Multidimensional Scaling

MDS is a computational method for determining and visualizing the similarities or dissimilarities (distances) between objects in a dataset [20]. The main concept is to find the key dimensions explaining the observed distances between the objects. The matrix $\mathbf{D}$ is the source of information of the MDS. The algorithm tries to find the positions of $M \leq P$ dimensional objects $\widehat{\mathbf{v}}_i$ (represented by points), producing a matrix $\widehat{\mathbf{D}} = [d(\widehat{\mathbf{v}}_i, \widehat{\mathbf{v}}_j)]$ that approximates the original one. Several MDS types were proposed and we can cite the metric, non-metric, and generalized versions. For the metric MDS, we have minimization of the stress cost function $\mathcal{S}$:

$$\mathcal{S} = \left[\sum_{i<j} \left[d(\mathbf{v}_i, \mathbf{v}_j) - d(\widehat{\mathbf{v}}_i, \widehat{\mathbf{v}}_j)\right]^2\right]^{\frac{1}{2}}. \tag{12}$$

The Sammon criterion can be also adopted, yielding:

$$\mathcal{S} = \left[\frac{\sum\limits_{i<j} \left[d(\mathbf{v}_i, \mathbf{v}_j) - d(\widehat{\mathbf{v}}_i, \widehat{\mathbf{v}}_j)\right]^2}{\sum\limits_{i<j} \left[d(\mathbf{v}_i, \mathbf{v}_j)\right]^2}\right]^{\frac{1}{2}}. \tag{13}$$

The stress S has a monotonic decreasing variation with the dimension M. The user establishes a compromise between the two variables, and usually either $M = 2$ or $M = 3$ is adopted since such values allow a direct graphical representation. The resulting map is read by following the clusters and by checking how they reflect the relationships embedded in the original data. Consequently, the shape of the map and the dimensions of the locus are meaningless.

For assessing the "quality" of the MDS, the user can check, subjectively, whether the locus clearly displays some clusters reflecting the characteristics of the dataset. Additionally, the user can compare the original and the reproduced information stored in $\mathbf{D}$ and $\widehat{\mathbf{D}}$, respectively. The Shepard diagram portraits $d(\mathbf{v}_i, \mathbf{v}_j)$ versus $d(\widehat{\mathbf{v}}_i, \widehat{\mathbf{v}}_j)$, so that a good representation corresponds to points close to the 45 degree line. Alternatively, the plot of S versus M indicates a good representation when we have a significant reduction of the stress. If the map is not clear the user can adopt another measure $d(\mathbf{v}_i, \mathbf{v}_j)$ until obtaining a suitable representation.

Similarly to the HC, the definition of an adequate distance $d(\mathbf{v}_i, \mathbf{v}_j)$ requires some practice and eventually a few numerical trials. We must note that the alternative distances are correct, the difference being merely in the capability of each one to capture the characteristics embedded in the dataset.

Several distances can lead to valid MDS maps and reveal the same clusters, just differing in their geometrical shapes.

2.4. Spectral Domain

Let us consider the time-series $\mathcal{X} = \{x_n : n = 1, \ldots, N\}$, resulting from sampling a continuous variable $x(t)$ at the frequency f_s. We can express $\mathcal{X}$ in the frequency-domain using the discrete Fourier transform, resulting in:

$$\mathcal{Y} = \{y_k : k = 1, \ldots, N\} = \mathcal{F}\{\mathcal{X}\}, \tag{14}$$

$$y_k = \sum_{n=1}^{N} x_n e^{-\imath \frac{2\pi}{N}(k-1)(n-1)}, \tag{15}$$

where $\imath = \sqrt{-1}$ and $\mathcal{F}\{\cdot\}$ is the Fourier operator. Often, we consider only the first half of the spectrum versus frequency, f, by considering $k = 1, \ldots, \left\lceil \frac{N}{2} \right\rceil$ and $f = k\frac{F_s}{2} / \left\lceil \frac{N}{2} \right\rceil$, where $\lceil \cdot \rceil$ stands for the ceiling function.

2.5. Entropy

Let us consider a discrete probability distribution $\mathbf{P} = \{p_1, p_2, \ldots, p_N\}$, with $\sum_i p_i = 1$ and $p_i \geq 0$. The Shannon entropy, $H^{(S)}$, of $\mathbf{P}$ is given by:

$$H^{(S)} = \sum_i p_i I(p_i) = -\sum_i p_i \ln p_i, \tag{16}$$

which represents the expected value of the information content $I(p_i) = -\ln p_i$.

Several generalizations of (16) have been proposed [21]. Herein, we recall the Machado—$H_\alpha^{(M)}$ [22], and Machado and Lopes—$H_{q,\alpha}^{(ML_1)}$ and $H_{q,\alpha}^{(ML_2)}$ [21], formulations, derived in the framework of fractional calculus (FC). The FC generalizes the concepts of differentiation [23–26] to non-integer orders. The theory was introduced by Leibniz by the 17th century, but only recently gained popularity in applied sciences [27–33].

The derivation of $H_\alpha^{(M)}$ starts from viewing the Shannon information $I(p_i) = -\ln p_i$ as a function lying between $D^{-1}I(p_i) = p_i(1 - \ln p_i)$ and $D^1 I(p_i) = -\frac{1}{p_i}$, where D^α stands for the fractional derivative of order $\alpha \in \mathbb{R}$. Therefore, the concepts of fractional information and fractional entropy of order α can be formulated as:

$$I_\alpha(p_i) = D^\alpha I(p_i) = -\frac{p_i^{-\alpha}}{\Gamma(\alpha + 1)}\left(\ln p_i + \widetilde{\psi}\right), \tag{17}$$

$$H_\alpha^{(M)} = \sum_i \left[-\frac{p_i^{-\alpha}}{\Gamma(\alpha + 1)}\left(\ln p_i + \widetilde{\psi}\right) \right] p_i, \tag{18}$$

where $\widetilde{\psi} = \psi(1) - \psi(1 - \alpha)$ and $\psi(\cdot)$ represents the digamma function. For the case $\alpha = 0$, we verify that $H_\alpha^{(M)}$ yields the Shannon entropy $H^{(S)}$.

For the derivation of $H_{q,\alpha}^{(ML_1)}$ and $H_{q,\alpha}^{(ML_2)}$, we adopt a general averaging operator, instead of the linear one that is assumed for the Shannon entropy (16). Let us consider a monotonic function $f(x)$ with inverse $f^{-1}(x)$. Therefore, for a set of real values $\{x_i\}$, $i = 1, 2, \ldots$, with probabilities $\{p_i\}$, we can define a general mean [34] associated with $f(x)$ as:

$$f^{-1}\left(\sum_i p_i f(x_i)\right). \tag{19}$$

Applying (19) to the Shannon entropy (16) we obtain:

$$H = f^{-1}\left(\sum_i p_i f(I(p_i))\right), \tag{20}$$

where $f(x)$ is a Kolmogorov–Nagumo invertible function [35]. If the postulate of additivity for independent events is considered in (19), then only two functions $f(x)$ are possible, consisting of $f_1(x) = c \cdot x$ and $f_2(x) = c \cdot \exp[(1-q)x]$, with $c, q \in \mathbb{R}$. For $f_1(x)$ we get the ordinary mean and we verify that $H = H^{(S)}$. For $f(x) = c \cdot e^{(1-q)x}$ we have the expression:

$$H = \frac{1}{1-q}\sum_i p_i \cdot \exp[(1-q)I(p_i)], \tag{21}$$

leading to the Rényi entropy:

$$H_q^{(R)} = \frac{1}{1-q}\ln\left(\sum_i p_i^q\right),\ q > 0, q \neq 1. \tag{22}$$

If we combine (17) and (21), then we obtain:

$$\begin{aligned} H_{q,\alpha}^{(ML_1)} &= \frac{1}{1-q}\ln\left\{\sum_i p_i \cdot \exp\left[(1-q)\cdot I_\alpha(p_i)\right]\right\} \\ &= \frac{1}{1-q}\ln\left\{\sum_i p_i \cdot \exp\left[(q-1)\cdot \frac{p_i^{-\alpha}}{\Gamma(\alpha+1)}\left(\ln p_i + \widetilde{\psi}\right)\right]\right\}. \end{aligned} \tag{23}$$

On the other hand, if we rewrite (22) as:

$$\begin{aligned} H_q^{(R)} &= \frac{q}{1-q}\ln\left[\left(\frac{1}{N}\sum_i p_i^q\right)^{\frac{1}{q}} \cdot N^{\frac{1}{q}}\right] \\ &= \frac{q}{1-q}\ln\left[\langle p_i\rangle_g \cdot N^{\frac{1}{q}}\right], \end{aligned} \tag{24}$$

where $\langle p_i\rangle_g = \left(\frac{1}{N}\sum_i p_i^q\right)^{\frac{1}{q}}$ is a generalized mean, then we obtain:

$$H_{q,\alpha}^{(ML_2)} = D^\alpha H_q^{(R)} = \frac{1}{N^{\frac{\alpha}{q}}}\frac{q}{1-q}\left[\frac{\langle p_i\rangle_g^{-\alpha}}{\Gamma(\alpha+1)}\left(\frac{1}{q}\ln N + \ln\langle p_i\rangle_g + \widetilde{\psi}\right)\right]. \tag{25}$$

In the limit, when $\alpha \to 0$, both $H_{q,\alpha}^{(ML_1)}$ and $H_{q,\alpha}^{(ML_2)}$ yield (22).

3. The Spans of Wars

This Section characterizes the real-world data describing the spans of wars. In Section 3.1 the adopted dataset is presented. In Section 3.2 these data are processed by computing the dissimilarity indices (1)–(27), followed by the HC and the MDS techniques for dimensionality reduction and scientific visualization. The loci are interpreted in the light of the emerging clusters.

3.1. Description of the Dataset

Wars have resulted in about 3.5 billion casualties, people who died in the battlefields or later on, as an indirect consequence or a result of those events. Since 1820, ninety five international and intra-state wars have occurred, depending on how war is defined [36,37].

Table A1, in Appendix A, contains the database of military conflicts from century VI B.C. to present date that is considered in this paper. Its construction adhered to a strict and prudent account of proceedings in order to preserve scholarly caution in synthesizing the conflicts whose consequences can be measured by the suffering that results. The selection criterion was based on the threshold of 25,000 estimated casualties, because this indicator can express not only lost human capital, but also its devastating impact on families and society in terms of pain and social disruption [38]. The database is global, as it includes all military conflicts above the defined threshold of casualties, wherever they took place. The number of casualties, namely, for ancient conflicts, is derived from historical texts by contemporary writers. For some wars, deaths due to collateral effects are included, such as those due to diseases caused by starvation and general degradation of health care. For details, please refer to the notes in Table A1.

The database contains $N = 163$ wars, where the ith war, $i = 1, \ldots, 163$, is characterized by means of four variables: (i) the mean (or center) time of the event, $t_i = \frac{t_{b_i} + t_{e_i}}{2}$, where t_{b_i} and t_{e_i} denote the starting and ending years, respectively; (ii) the time span, $T_i = t_{e_i} - t_{b_i} + 1$ (expressed in years); (iii) the number of belligerents, B_i; and (iv) the number of deaths, C_i. Therefore, the data are organized in a 163×4 dimensional array, $\widetilde{\mathbf{W}} = [\widetilde{w}_{ik}]$, where $\widetilde{w}_{ik}$, $i = 1, \ldots, 163$, $k = 1, \ldots, 4$, represents the ith war and its kth characterizing variable.

3.2. The HC Analysis and Visualization of the Spans of Wars

For applying the HC, firstly the array $\widetilde{\mathbf{W}}$ is normalized by the arithmetic mean, $\mu(\cdot)$, and standard deviation, $\sigma(\cdot)$, to avoid numerical saturation. This means that the columns of $\widetilde{\mathbf{W}}$, to be denoted by $\widetilde{\mathbf{u}}_k$, are converted to:

$$\mathbf{u}_k = \frac{\widetilde{\mathbf{u}}_k - \mu(\widetilde{\mathbf{u}}_k)}{\sigma(\widetilde{\mathbf{u}}_k)}, \tag{26}$$

yielding a normalized array $\mathbf{W}$. Secondly, the rows of $\mathbf{W}$, to be denoted by $\mathbf{v}_i$, are used for calculating the dissimilarity matrices $\mathbf{D}_n = [d_n(\mathbf{v}_i, \mathbf{v}_j)]$, $i, j = 1, \ldots, 163$, where $d_n(\mathbf{v}_i, \mathbf{v}_j)$ denotes one distance in the set $\{d_1, \ldots, d_9\}$. Finally, the matrices $\mathbf{D}_n$ are processed through the HC for producing the loci of objects that represent the spans of wars. The agglomerative clustering and average-linkage methods are adopted.

Although the HC trees are 2-dimensional loci, we can highlight particular aspects embedded in the data or capture distinct information provided by the HC. Herein, the HC trees will consist of two dimensions produced by the standard HC and one extra dimension, corresponding to time, t, or casualties, C. The 3rd dimension is thus obtained by means of radial basis interpolation (RBI) [39], using the information of each point and the thin-plate spline $\phi(\epsilon) = \epsilon^2 \log \epsilon$, where ϵ stands for the Euclidean distance between the HC points in the plane. Therefore, isoclines represent identical loci of time or of casualties.

Figures 1 and 2 depict, for example, the HC trees obtained with the Jaccard and Sørenson distances, d_6 and d_9, respectively, while the 3rd dimension is calculated interpolating either t or $\ln(C)$. For the other distances the loci are of the same type. For both distances, we verify the emergence of identical clusters, $\mathcal{C}_1$ and $\mathcal{C}_2$, composed by sub-clusters, $\mathcal{C}_{11}$ and $\mathcal{C}_{12}$, and $\mathcal{C}_{21}$ and $\mathcal{C}_{22}$, respectively. These clusters reflect the similarities between objects, but often the interpretation of the loci is difficult, namely, in the presence of many objects.

Figure 3 shows the Shepard plot for assessing the HC tree with the distance d_6. The chart reflects an accurate clustering of the original data, with $cc = 0.89$. For the other distances the charts are identical, and therefore, are not presented.

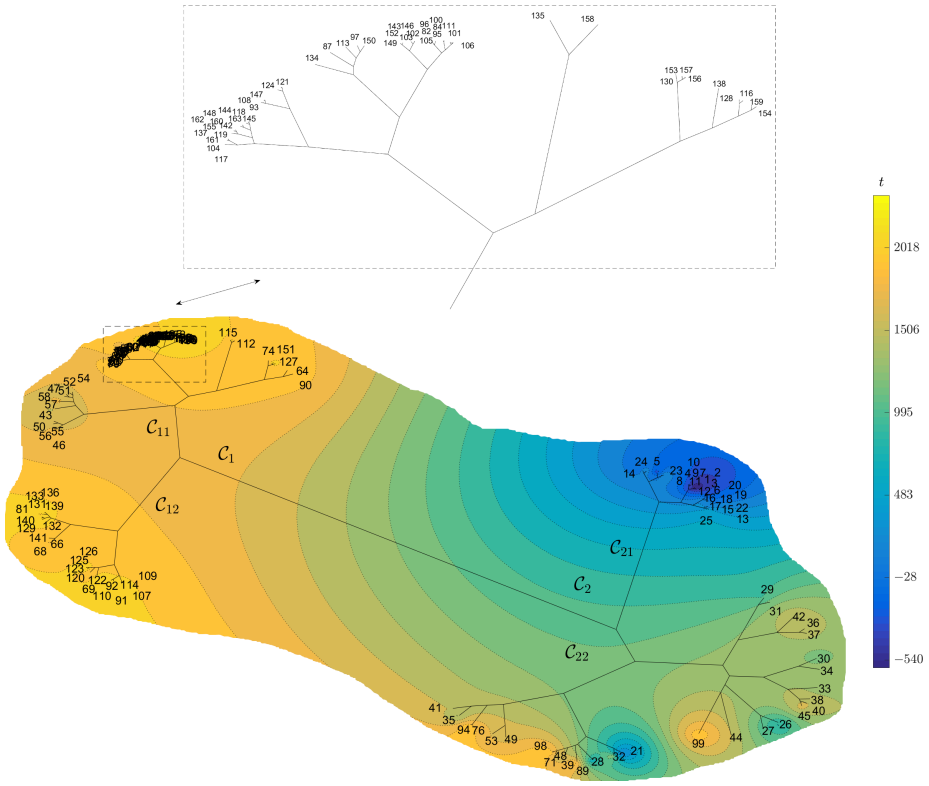

(**a**)

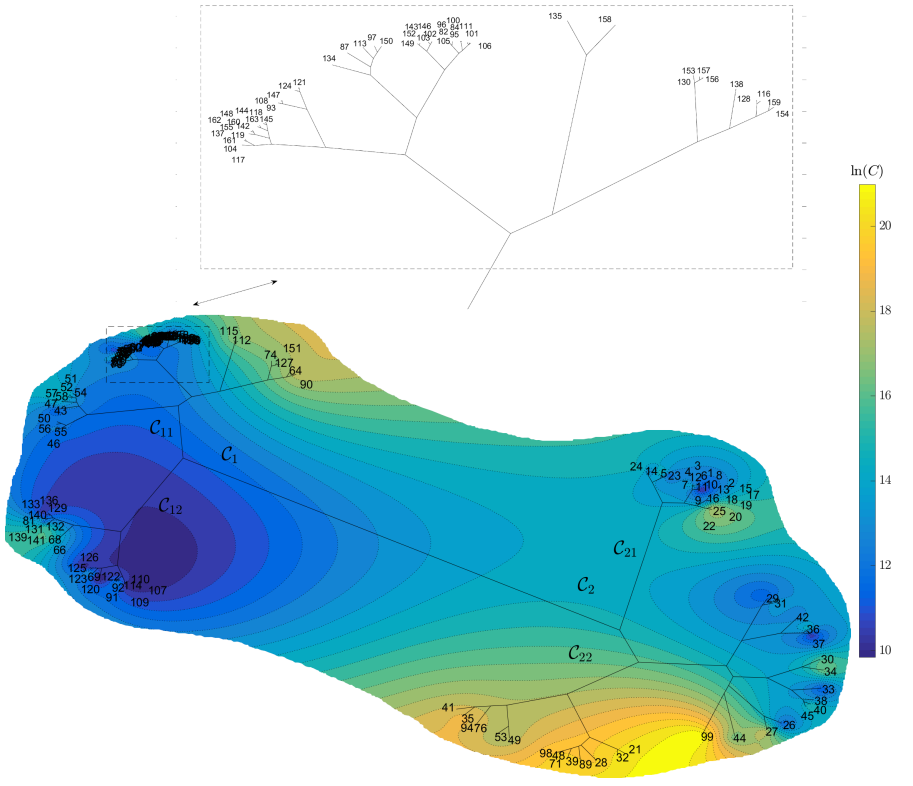

(**b**)

Figure 1. The hierarchical trees obtained with the Jaccard distance, d_6, and the 3rd dimension calculated by RBI based on: (**a**) time (year), t; (**b**) logarithm of the casualties, that is, $\ln(C)$. A magnification of the denser part is included.

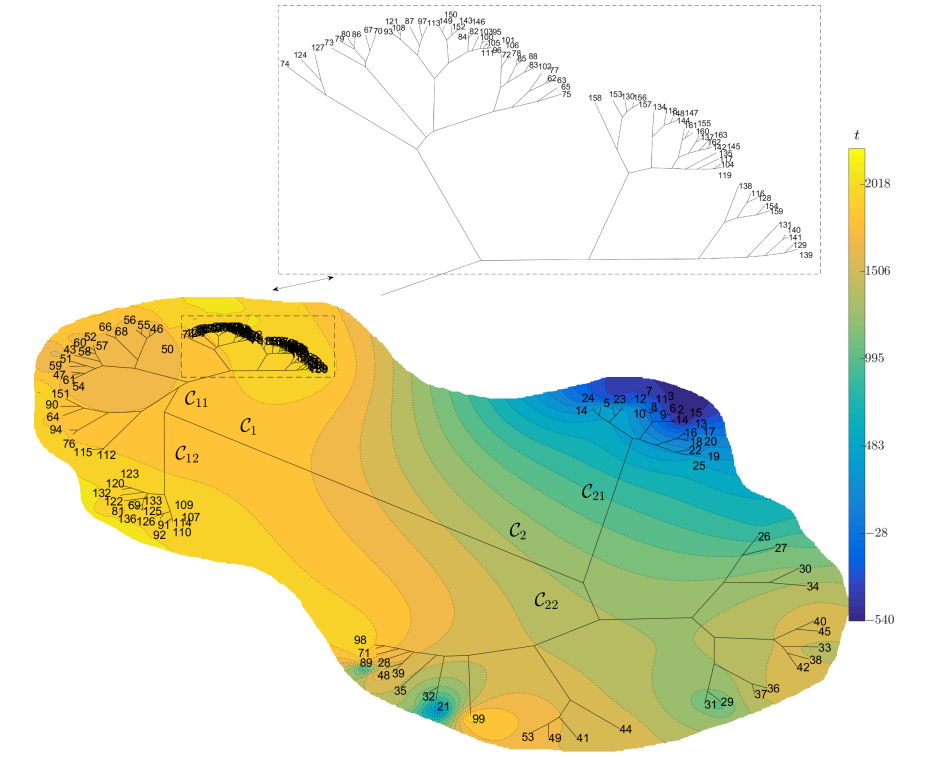

(**a**)

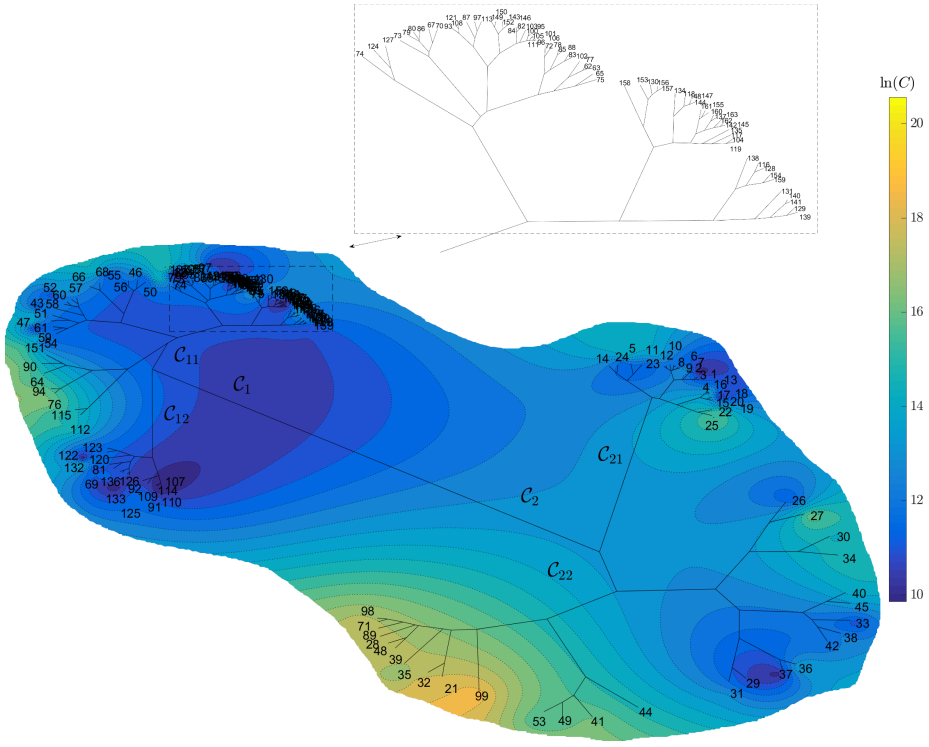

(**b**)

Figure 2. The hierarchical trees obtained with the Sørenson distance, d_9, and the 3rd dimension calculated by RBI based on: (**a**) time (year), t; (**b**) logarithm of the casualties, that is, $\ln(C)$. A magnification of the denser part is included.

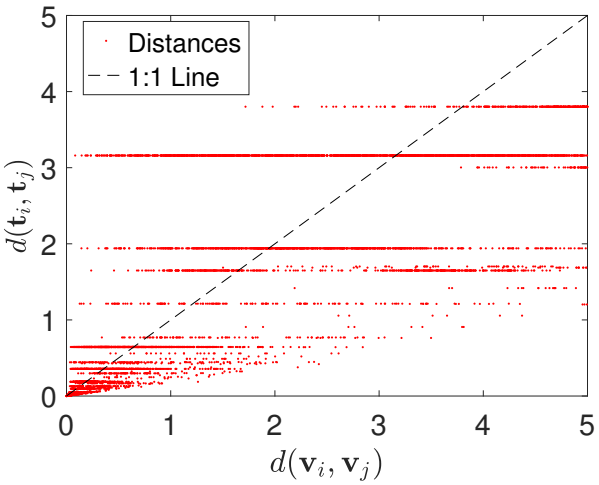

Figure 3. Shepard plot for the HC cophenetic distances obtained with d_6. The cophenetic correlation coefficient is $cc = 0.89$.

3.3. The MDS Analysis and Visualization of the Spans of Wars

We visualize the spans of wars using the metric MDS and the Sammon criterion (13). The inputs to the algorithm are the matrices $\mathbf{D}_n$. Figures 4 and 5 depict, for example, the 3-dimensional MDS loci obtained with the Jaccard and Sørenson distances, d_6 and d_9, respectively. The spheres representing wars have sizes proportional to the numbers of casualties, and color is proportional to time. Figure 6a,b shows the MDS assessment charts for the Jaccard distance. Since the Shepard diagram exhibits a small scatter around the 45 degree line, we have a good fit between the initial and reproduced distances $d_6(\mathbf{v}_i, \mathbf{v}_j)$ and $d_6(\widetilde{\mathbf{v}}_i, \widetilde{\mathbf{v}}_j)$. The stress plot shows that the 3-dimensional locus is a good representation, since $M = 3$ points to the elbow of the function $\mathcal{S}(M)$. Therefore, 3-dimensional representations give a good compromise between accuracy and readability. For the other distances we obtain charts of the same type.

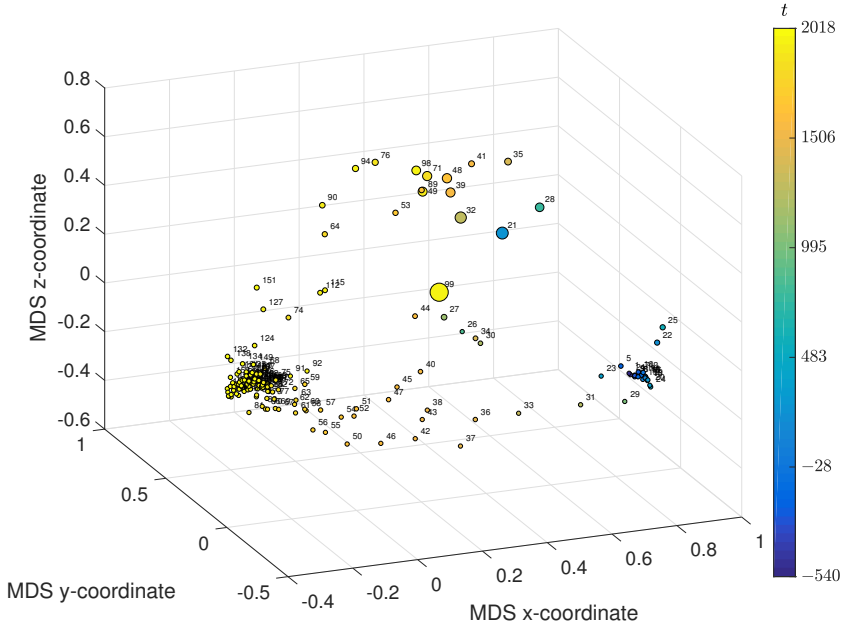

Figure 4. The 3-dimensional MDS loci obtained with the Jaccard distance, d_6. The spheres represent wars, with size proportional to the number of casualties, C, and color is proportional to time (years), t.

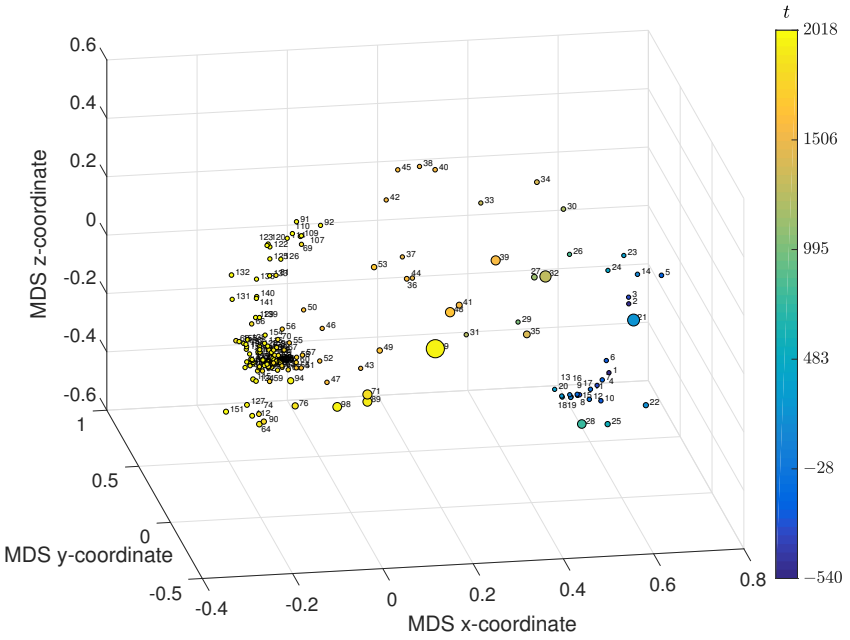

Figure 5. The 3-dimensional MDS loci obtained with the Sørenson distance, d_9. The spheres represent wars, with size proportional to the number of casualties, C, and color proportional to time (years), t.

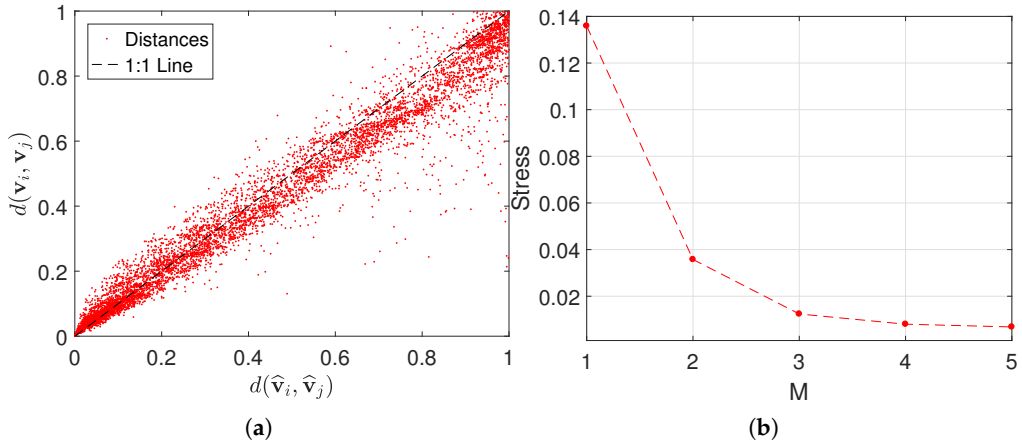

Figure 6. The MDS assessment charts for the Jaccard distance, d_6: (**a**) Shepard; (**b**) stress.

3.4. The MDS Analysis and Visualization of the Spans of Wars based on a Generalized Distance

Distances (1)–(9) have their own pros and cons; that is to say, they highlight specific aspects of the data, but give lesser importance to others. Therefore, in order to embed their distinct characteristics, we propose the distance d_{10} as "generalized":

$$d_{10}(\mathbf{v}_i, \mathbf{v}_j) = \sum_{r=1}^{9} \lambda_r \frac{d_r(\mathbf{v}_i, \mathbf{v}_j)}{\max[d_r(\mathbf{v}_i, \mathbf{v}_j)]}, \tag{27}$$

where $\lambda_r \in \mathbb{R}$, $\sum_{i=1}^{9} \lambda_r = 1$, are weighting constants.

In other words, we conjecture that the distances (1)–(9) capture distinct characteristics of the objects and that a more complete grasp of the information is obtained by using all indices complementarily. Therefore, distance (27) may lead to a multi-perspective visualization. Since we have no a priori preference for a given distance we consider in the follow-up all weights to be identical, that is, $\lambda_r = \frac{1}{9}$, $r = 1, \ldots, 9$.

Figure 7 depicts the 3-dimensional MDS loci obtained with the generalized distance, d_{10}. The spheres size and color have the same meaning as in the previous MDS loci. The corresponding MDS assessment charts are omitted, since they are of the same type as those shown in Figure 6.

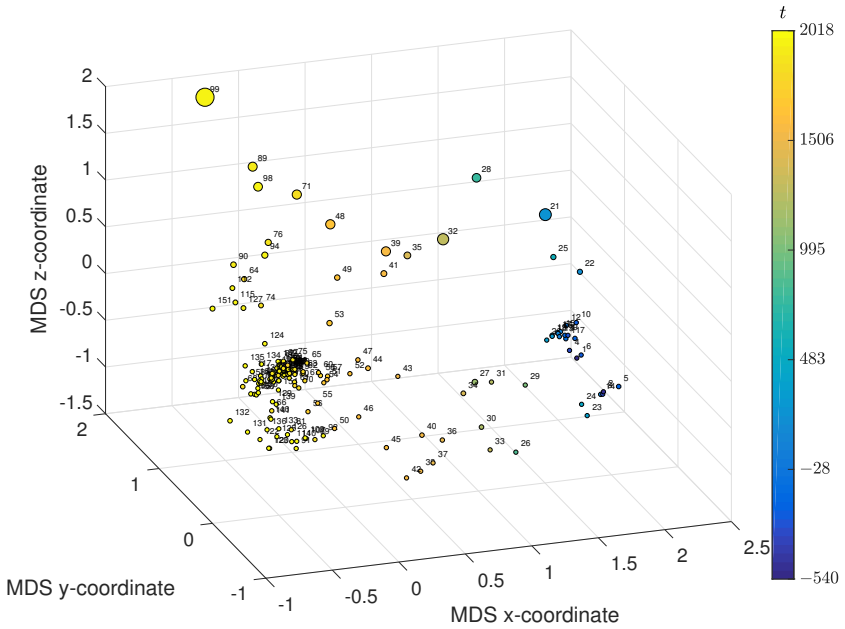

Figure 7. The 3-dimensional MDS loci obtained with the generalized distance, d_{10}. The spheres represent wars, with size proportional to the number of casualties and color proportional to time.

Several experiments showed that, as expected, the generalized distance, d_{10}, leads to better clustering than the one revealed by the distances $\{d_1, \ldots, d_9\}$ used separately. More importantly, we note in all cases, the explosion in the number of events during the recent decades and a large scattering in the MDS plots for the events in the last decades corresponding to a multitude of distinct characteristics.

4. Sociological Interpretation of the Spans of Wars

Perhaps wars are as ancient as humankind, and go back for tens or hundreds of thousands of years, because they are of great value in clarifying the human responses to disputes. During the Mesolithic period, from circa 9700 B.C. to 8750 B.C., when European hunter-gatherers settled and developed more complex societies, they developed warring. However, they are not considered in Table A1, because collective memory on these wars has been lost, as writing systems were not available and oral tradition has given origin to only myths and legends.

Causes for warring in sedentary existence also include the shift to a growing population, and concentrations of assets and value in terms of resources such as livestock, which have increased the complexity of social relationships and social ranking. Cooperation in hunting, agriculture, or food sharing must be recognized as means for conflict resolution. The existence of surpluses triggered barter for common products and trade in high-value commodities. Both Europeans and Asians faced scarcity of resources in Ancient ages. From the 6th century B.C. to the 4th century A.D., 24 military events took place in 11 centuries, which averages to one every 50 years. The 24 ancient wars here represented with a frequency of one per half a century make a cluster of their own (Figure 7). The establishment of collective identities required group boundaries and territory control in the Chinese, Greek, Persian, and Roman empires. The Three kingdom war (labeled with number 21) from the Han to the Jin dynasty, and the Yellow Turban Rebellion (labeled with number 22) are the bloodiest known conflicts since the beginning of humankind.

Splitting of empires also brought military conflicts, such as the Hunnic invasions which put an end to the West Roman empire (with number 24 in Figure 7). The flexibility that allowed individuals to move to other groups was another superior instrument for social and political arrangements. Such peaceful social mechanisms have included family alliances through marriage, and cross-group ties of kinship. However, these mechanisms did not eliminate serious conflict, namely, because of religion or ideological mass killings, such as Reconquista from the Muslims and the Crusades (1095–1291), labeled in the Figure 7 as 27. Territorial conquest and economic gain continued as the bloodiest, such as the Mongol conquests (32 in the Figure 7, in the cloud), and the Timured Conquests (35) which downgrade the importance of the European Hundred Years' War (34 in the cloud). Clouds mean that peaceful periods occurred for short duration. The long durations of these kinds of wars for control of means of production, trade routes, and raw materials oblige belligerents to invest great amounts of spending and armies' blood, which makes it very difficult to stop fighting if victory is not clear, because losses would become useless [40]. Continuation of fighting is the way to redeem all previous military efforts and human sacrifices.

There was also a tremendous dependency on weather conditions. According to rainfalls, temperature, and other weather conditions, crops could flourish or be lost. Production was subject to high vulnerability, and standards of life could deteriorate because of scarcity, high pricing of food, and diet problems for a large number of people. Under those conditions, standards of life could languish, and resistance to diseases could decrease, soon resulting in famine, epidemics, and higher mortality, as happened because of the Eurasian Black Death epidemics (1343–1353). Riots, revolts, and warring were a common consequence of such a set of difficult conditions for human survival. Expansion to scarcely known lands, in the Modern Age, brought discovery and colonization. Wars labeled 37 to 61 were the great Modern Age wars. The Spanish conquests of Yucatan, the Inca, and the Azteca empires in the New World (which are labeled as 39 to 41 Figure 7) are famous, which downgrades the European conflicts (such as the French Wars of Religion labeled 44, and the Thirty Years' War labeled 49) [41] thanks to the spread of diseases in the New World [42]. Strategic innovations became available for military superiority, and new hopes supported victory possibilities [43]. The old armor, pikes, and longbows became old fashioned when compared to muskets and cannons, increasing human sacrifice (casualties), as Figure 7 clearly shows [43].

Environmental and economic conditions strongly conditioned "the economic history of man as a successful species" [44]. A good example of the correlation between bad weather conditions and lower production levels did happen in the 17th century in Northern Europe. The so-called Cooling age generated conditions that led to wars (labeled 49–52, 54–57, and 59 and 60). Environmental upheavals such as long rainy winters obliged an adaptation to alternative means of survival beyond colonial expansion: capitalist industry, trading, and finance. A world without water or ice is hard to visualize, and recent trends toward increasing average temperatures may bring serious problems to humankind, and military conflicts may also become more plausible and frequent [45].

Looking at contemporary history, newly available and sophisticated means of warfare became available in this phase. Artillery and bombing at a distance were key aspects in Napoleon's invasions and conquest wars, (labeled 64 in the Figure 7). Soldiers' bodies engaged one another within confined battlefields has given place to long-range weapon technologies. Wars became much bloodier in the nineteenth and twentieth centuries. Civil wars have dominated the military scene, and the Chinese Civil War of 1927-49 downgraded the American and the Spanish Civil Wars (1861-65 and 1936-39, respectively) with labels 75 and 97.

More recently, the World Wars' modern battlefields labeled 89 and 99 also differed a lot, because of the air force bombing capacity in the second one (1939–1945). By earlier standards, the First World War (1914–1918), was not in fact particularly global [46]. Recent weaponry technology has evolved in two different aspects: destructiveness and distance. Each one of the most recent wars was dramatically bloody (colored yellow-orange-green in Figures 1, 2, 4, 5, and 7. Weapons with great destructive power

can defeat any enemy nowadays (or at least oblige its government to sit for a bargaining deal). By operating across great distances, they present much higher effective ranges of threat.

Global-scale ambition and conquest purposes have been explanatory variables for more frequent belligerency. Such a high frequency of conflict means that it has been difficult to reap the anticipated gains that were forecast for victory [47]. Perhaps the announcements of messianic future benefits of victory by ruling elites and their political propaganda frequently have been persuasive so as to create popular domestic attitudes of enthusiasm and support to fighting. The return to peace and normalcy includes tremendous political costs for politicians, even for victors.

5. Entropy Analysis of the Span of Wars

The number of casualties in each war, C_i, $i = 1, \ldots, N$, with $N = 163$, is distributed along the time span, $T_i = t_{e_i} - t_{b_i} + 1$, yielding the "density of casualties" time-series:

$$\mathcal{X} = \{x_n : n = t_{b_1}, \ldots, t_{e_N}\} = \sum_{i=1}^{N} \sum_{n=t_{b_i}}^{t_{e_i}} \frac{C_i}{T_i} \delta(n), \tag{28}$$

where t_{b_i} and t_{e_i} stand for the beginning and the end the ith war, respectively, and $\delta(n)$ denotes the Dirac delta function at time n.

Figure 8 depicts the time-series $\mathcal{X}(n)$ and its spectrum $|\mathcal{Y}(f)|$. In the first, we note the tendency toward chaotic-like behavior, and in the second, we verify the existence of some complex behavior. Therefore, we need some more assertive mathematical and numerical tool to unveil other characteristics of the dataset.

We start by adopting a 10-year sliding window without overlap, that is, slicing the time-series $\mathcal{X}$ into 275 intervals, w_i $(i = 1, \ldots, 275)$. This minimizes issues related to the non-stationarity of the data and yields a good compromise between time discrimination and statistical significance. For the ith window we determine a histogram by binning the elements of w_i into 10 equally spaced containers and counting the number of elements in each container. Then, we compute the Shannon and fractional entropies discussed in Sections 2.4 and 2.5, where the probabilities are estimated from the histograms of relative frequencies.

Figure 9 depicts the results, where the parameter $q = 1.2$ and the fractional order are $\alpha = \{0.3, 0.3, -0.2\}$ for $H_\alpha^{(M)}$, $H_{q,\alpha}^{(ML_1)}$ and $H_{q,\alpha}^{(ML_2)}$, respectively. For these values, the fractional entropies have a higher sensitivity to the data characteristics [21].

The two models:

$$f_1 = 1 - e^{-\beta_1 n - \beta_2 n^2 - \beta_3 n^3 - \beta_4 n^4} \tag{29}$$

and

$$f_2 = \beta_1 + (1 - \beta_1) \left(1 - e^{-\beta_2 n - \beta_3 n^2 - \beta_4 n^3}\right), \tag{30}$$

fit well into $\left\{H^{(S)}, H_\alpha^{(M)}\right\}$ and $\left\{H_{q,\alpha}^{(ML_1)}, H_{q,\alpha}^{(ML_2)}\right\}$, respectively, where $\{\beta_1, \beta_2, \beta_3, \beta_4\} \in \mathbb{R}$ are the models' parameters, whose values are listed in Table 1.

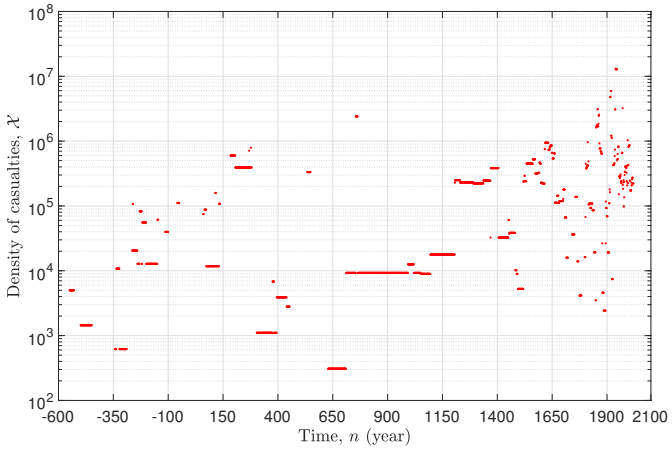

(a)

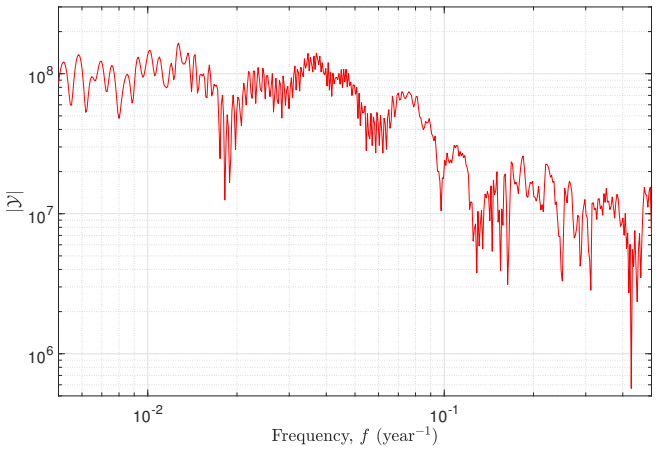

(b)

Figure 8. The density of casualties and its spectrum: (**a**) $\mathcal{X}(n)$; (**b**) $|\mathcal{Y}(f)|$.

Table 1. Values of the parameters $\{\beta_1, \beta_2, \beta_3, \beta_4\}$ for the fitting models of $H^{(S)}$, $H_\alpha^{(M)}$, $H_{q,\alpha}^{(ML_1)}$ and $H_{q,\alpha}^{(ML_2)}$.

	β_1	β_2	β_3	β_4
$H^{(S)}$	1.540×10^{-2}	-1.062×10^{-4}	-3.918×10^{-7}	2.914×10^{-9}
$H_\alpha^{(M)}$	-1.250×10^{-2}	2.377×10^{-4}	-1.90×10^{-6}	4.921×10^{-9}
$H_{q,\alpha}^{(ML_1)}$	-1.147	1.127×10^{-2}	-1.353×10^{-4}	4.205×10^{-7}
$H_{q,\alpha}^{(ML_2)}$	-7.503	3.354×10^{-3}	-3.670×10^{-5}	1.019×10^{-7}

We clearly observe three periods: the first, $\mathcal{P}_1 \in [-549, 650]$, with a slow increase of the entropy until the middle followed by a slow decreasing; the second, $\mathcal{P}_2 \in [650, 1400]$, with very small values of entropy; and the third, $\mathcal{P}_2 \in [1400, 2020]$, with a fast increase of the entropy. This behavior is coherent with the explosion of conflicts with large mortality rates fueled by the development of more "efficient" weapons. In fact, guided missiles and sniper fire (and drones, nowadays) are allowing targeting more enemies and economic resources, with lower risk of counterattacks. The aftermath of a war has always included disaster, economic disarray, and profound social unrest for the defeated partners, with unbearable costs beyond the efforts in belligerency. More importantly, the results highlight an evolution toward increasing values of the entropy, somehow reflecting a thermodynamic behavior, seemingly aligned with the anthropological and social issues pointed out in this paper. This conclusion was also reached previously based on different concepts and tools, namely, when using HC and MDS

for a collection of distances. Therefore, the results obtained by distinct techniques are compatible and seem not to depend on the type of measure or the computational approach hand. Moreover, we verify that a data-driven modeling, combining mathematical and computational tools, constitutes a relevant exploratory strategy for describing complex real-world phenomena. Indeed, we are tackling a class of systems for which a classical approach based purely on an analytical perspective would require subjective initial assumptions, possibly biasing the resulting analysis.

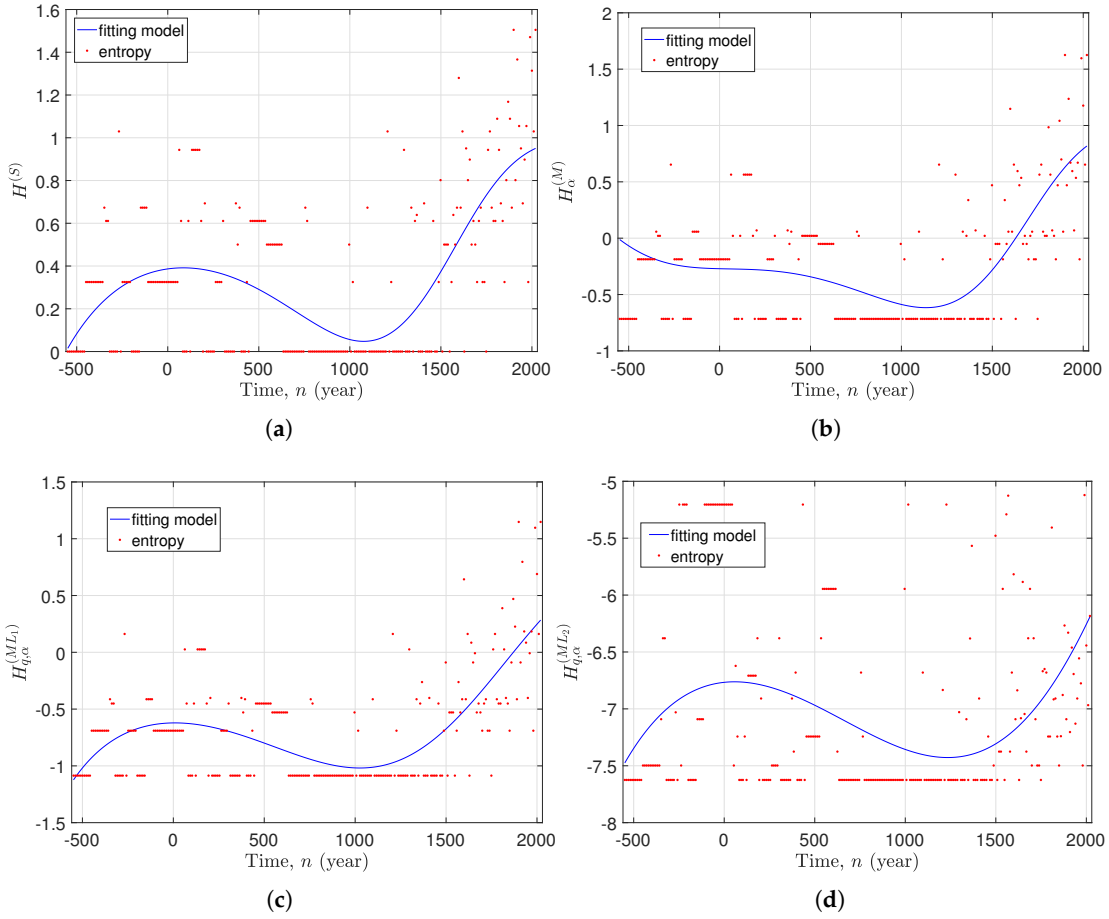

Figure 9. Entropy versus window, w_i: (**a**) $H^{(S)}$; (**b**) $H_{\alpha}^{(M)}$, $\alpha = 0.3$; (**c**) $H_{q,\alpha}^{(ML_1)}$, $\{q, \alpha\} = \{1.2, 0.3\}$; (**d**) $H_{q,\alpha}^{(ML_2)}$, $\{q, \alpha\} = \{1.2, -0.2\}$.

6. Discussion and Conclusions

MSD revealed the entire graphical appraisal of humankind's warring. When looking at the historical record of wars, one can see that warring is not an abnormality for the humankind. From a long-term perspective, warring may be equated as a powerful element in the economic history of the humankind, as military defeat means the spoiling of economic resources (including loss of human capital) beyond social turmoil.

War has served as a mechanism of natural selection in which the fittest prevailed to acquire both mates and resources. Ravaged economies and societies have had great difficulties to return to growth, while military victory for their enemies brought enlargement of territory and more availability of economic and human resources. Warship may be an instrument of policy for reaching economic targets from a strategical perspective, a kind of investment for expansionary purposes in a local, regional, or global context. War is a deliberate and instrumental economic choice of political and military elites for leadership. In a distinct perspective, we verified that present day computational techniques, both for data processing, and for visualization of the results, may represent a key role in the study of

these dramatic events. This strategy does not preclude the use of classical modeling techniques and in fact can be complemented by such description. Moreover, the proposed method suggests collecting further characteristics of the events since the algorithmic approach can easily handle a higher and richer description involving a higher number of dimensions.

On another level, we verified an increasing number of conflicts. This produced not only large scattering in the HC and MDS plots for recent times, but also larger and growing values of entropy. Such conclusions seem to be robust and not to depend on the mathematical index or computational tool. We can question ourselves whether human civilization is reflected by events such as wars that are manifestations of the second law of thermodynamics. The results seem to indicate that the Plato quote, "Only the dead have seen the end of war," is still going to be relevant for the years to come.

Author Contributions: J.A.T.M., A.M.L., and M.E.M. conceived, designed, and performed the experiments; analyzed the data; and wrote the paper. All authors have read and agreed to the published version of the manuscript.

Funding: This research received no external funding.

Conflicts of Interest: The authors declare no conflict of interest.

Appendix A

Table A1. List of 163 wars with more that 25,000 casualties (adapted from: https://en.wikipedia.org/wiki/List_of_wars_by_death_toll).

i	t_i	T_i	B_i	C_i	Name	Note
1	−540	20	4	100,000	Conquests of Cyrus the Great	Does not include civilian deaths (from texts by contemporary writers)
2	−474	51	2	73,800	Greco-Persian Wars	
3	−317	54	2	33,500	Samnite Wars	Does not include civilian deaths (from texts by Roman writers)
4	−330	14	4	142,000	Wars of Alexander the Great	Does not include civilian deaths (from texts by Greek writers)
5	−205	119	2	1,520,691	Punic Wars	
6	−253	24	2	185,000	First Punic War	Part of the Punic Wars
7	−210	18	2	770,000	Second Punic War	Part of the Punic Wars
8	−148	4	2	193,649	Third Punic War	Part of the Punic Wars
9	−262	2	2	173,205	Kalinga War	
10	−226	10	6	700,000	Qin's Wars of Unification	Part of Warring States Period
11	−107	13	3	516,236	Cimbrian War	Part of the Germanic Wars
12	−54	9	2	1,000,000	Gallic Wars	
13	61	2	2	150,000	Iceni Revolt	Part of the Roman Conquest of Britain. Year is uncertain.
14	101	71	2	836,660	Jewish-Roman Wars	
15	70	8	2	605,614	First Jewish-Roman War	Part of Jewish-Roman Wars
16	116	3	2	440,000	Kitos War	Part of Jewish-Roman Wars
17	134	5	2	481,664	Bar Kokhba Revolt	Part of Jewish-Roman Wars
18	269	1	2	320,000	Gothic War (269)	Part of the Germanic Wars
19	277	1	2	400,000	Probus's German War	Part of the Germanic Wars
20	379	7	2	40,000	Gothic War (376–382)	Part of the Germanic Wars
21	232	97	2	37,947,332	Three Kingdoms War	Includes the "unofficial" part of the Three Kingdoms period
22	195	22	2	4,582,576	Yellow Turban Rebellion	Part of Three Kingdoms War
23	372	136	2	150,000	Wars of the Sixteen Kingdoms	Does not include civilian deaths
24	424	59	2	165,000	Hunnic Invasions	Does not include civilian deaths (from texts by Roman writers).
25	541	15	2	5,000,000	Moorish Wars	
26	840	422	4	130,000	Arab-Byzantine Wars	Does not include civilian deaths (from texts by contemporary writers).
27	1102	782	4	7,000,000	Reconquista	
28	759	9	3	21,633,308	An Lushan Rebellion	
29	1006	27	2	90,000	Goryeo-Khitan Wars	
30	1193	197	4	1,732,051	Crusades	
31	1219	22	3	447,214	Albigensian Crusade	Part of the Crusades
32	1287	163	2	34,641,016	Mongol conquests	Does not include deaths due to the Black Death migration

Table A1. *Cont.*

i	t_i	T_i	B_i	C_i	Name	Note
33	1327	62	2	94,868	Wars of Scottish Independence	
34	1395	117	2	2,754,995	Hundred Years' War	
35	1388	36	4	12,649,111	Conquests of Timur	
36	1466	31	4	873,000	Conquests of Mehmed II "the Conqueror"	
37	1471	33	4	41,833	Wars of the Roses	
38	1527	66	4	346,410	Italian Wars	
39	1576	114	2	24,300,000	Spanish conquest of the Aztec Empire	Includes the cocoliztli plagues
40	1557	77	2	1,460,000	Spanish conquest of Yucatán	Includes deaths due to European diseases
41	1553	40	2	8,400,000	Spanish conquest of the Inca Empire	Includes deaths due to European diseases
42	1544	46	4	200,000	Campaigns of Suleiman the Magnificent	
43	1525	2	2	100,000	German Peasants' War	
44	1580	37	2	2,828,427	French Wars of Religion	
45	1608	81	5	648,074	Eighty Years' War	
46	1595	20	4	138,285	Anglo-Spanish War (1585–1604)	
47	1595	7	3	1,000,000	Japanese invasions of Korea	
48	1639	47	6	25,000,000	Qing conquest of the Ming	
49	1633	31	2	5,873,670	Thirty Years' War	
50	1647	25	4	200,000	Franco-Spanish War (1635–59)	
51	1645	13	4	876,000	Wars of the Three Kingdoms	
52	1647	10	2	511,527	English Civil War	Part of the Wars of the Three Kingdoms
53	1683	50	2	5,600,000	Mughal-Maratha Wars	
54	1675	7	4	220,000	Franco-Dutch War	
55	1691	17	4	120,000	Great Turkish War	
56	1711	22	4	350,000	Great Northern War	
57	1708	14	2	707,390	War of the Spanish Succession	
58	1746	11	2	400,000	Maratha expeditions in Bengal	
59	1760	8	4	1,102,361	Seven Years' War	
60	1767	5	2	70,000	Sino-Burmese War (1765–69)	
61	1779	9	4	37,324	American Revolutionary War	
62	1800	4	3	65,000	French campaign in Egypt and Syria	
63	1803	2	3	135,000	Saint-Domingue expedition	
64	1809	13	4	4,949,747	Napoleonic Wars	
65	1812	1	2	540,000	French invasion of Russia	Part of the Napoleonic Wars
66	1821	26	4	600,000	Spanish American Wars of Independence	
67	1817	14	2	228,000	Venezuelan War of Independence	Part of Spanish American Wars of Independence
68	1828	26	4	1,732,051	Mfecane	

Table A1. *Cont.*

i	t_i	T_i	B_i	C_i	Name	Note
69	1848	57	2	200,000	Carlist Wars	
70	1838	19	2	300,000	French conquest of Algeria	
71	1857	15	2	24,494,897	Taiping Rebellion	
72	1855	4	4	382,047	Crimean War	
73	1865	18	2	943,398	Panthay Rebellion	
74	1858	2	2	2,828,427	Indian Rebellion of 1857	
75	1863	5	2	806,226	American Civil War	
76	1870	16	3	9,797,959	Dungan Revolt	
77	1865	6	3	49,287	French intervention in Mexico	
78	1867	7	4	600,000	Paraguayan War	
79	1873	11	2	241,000	Ten Years' War	
80	1877	15	2	32,404	Conquest of the Desert	
81	1894	42	2	101,877	Aceh War	
82	1895	2	2	48,311	First Sino-Japanese War	
83	1897	4	3	362,000	Cuban War of Independence	
84	1901	4	2	120,000	Thousand Days' War	
85	1901	4	4	81,056	South African War (Second Boer War)	
86	1906	14	2	234,000	Philippine-American War	
87	1915	11	2	1,000,000	Mexican Revolution	
88	1913	2	4	140,000	Balkan Wars	
89	1916	5	27	23,568,559	World War I	
90	1920	6	4	6,708,204	Russian Civil War	
91	1961	86	4	210,784	Iraqi-Kurdish conflict	
92	1971	100	2	100,000	Kurdish rebellions in Turkey	
93	1928	10	2	40,000	Second Italo-Senussi War	
94	1938	23	2	9,671,401	Chinese Civil War	
95	1934	4	2	100,000	Chaco War	
96	1936	2	2	278,350	Second Italo-Ethiopian War	
97	1938	4	2	707,107	Spanish Civil War	
98	1941	9	5	22,360,680	Second Sino-Japanese War	Part of World War II
99	1942	7	193	69,069,811	World War II	
100	1940	2	2	173,071	Winter War	Part of World War II
101	1941	2	2	27,080	Greco-Italian War	Part of World War II
102	1943	4	3	387,333	Continuation War	Part of World War II

Table A1. *Cont.*

i	t_i	T_i	B_i	C_i	Name	Note
103	1945	1	3	56,574	Soviet-Japanese War	Part of World War II
104	1950	9	4	400,000	First Indochina War	
105	1948	4	2	158,000	Greek Civil War	
106	1948	2	2	35,000	Malagasy Uprising	
107	1984	74	2	93,808	Kashmir Conflict	
108	1953	11	2	193,697	La Violencia	
109	1984	73	2	180,278	Internal conflict in Myanmar	
110	1984	73	3	116,074	Arab-Israeli conflict	
111	1948	1	2	84,116	Indian annexation of Hyderabad	
112	1952	4	16	3,000,000	Korean War	
113	1958	9	2	724,569	Algerian War	
114	1987	67	3	34,000	Ethnic conflict in Nagaland	
115	1965	21	18	3,144,873	Vietnam War	
116	1964	18	2	500,000	First Sudanese Civil War	
117	1963	6	5	100,000	Congo Crisis	
118	1968	14	3	92,452	Angolan War of Independence	
119	1966	9	4	141,421	North Yemen Civil War	
120	1992	58	4	244,949	West Papua conflict	
121	1969	11	2	74,965	Mozambican War of Independence	
122	1992	57	7	25,000	Insurgency in Northeast India	
123	1992	57	4	220,000	Colombian conflict	
124	1969	4	2	1,732,051	Nigerian Civil War	
125	1994	51	3	120,000	Moro Conflict	
126	1995	52	2	35,917	CPP-NPA-NDF rebellion	
127	1971	1	2	3,000,000	Bangladesh Liberation War	
128	1983	18	2	866,025	Ethiopian Civil War	
129	1989	28	2	504,158	Angolan Civil War	
130	1983	16	4	134,164	Lebanese Civil War	
131	1991	33	4	100,000	Insurgency in Laos	
132	1999	43	4	1,574,802	War in Afghanistan	
133	1999	43	2	45,000	Kurdish-Turkish conflict	Part of the Kurdish rebellions in Turkey
134	1984	11	3	1,095,445	Soviet-Afghan War	Part of War in Afghanistan
135	1984	9	6	564,041	Iran-Iraq War	
136	2000	41	3	70,000	Internal conflict in Peru	
137	1984	6	3	223,607	Ugandan Bush War	

Table A1. *Cont.*

i	t_i	T_i	B_i	C_i	Name	Note
138	1994	23	2	1,414,214	Second Sudanese Civil War	
139	1996	27	2	89,443	Sri Lankan Civil War	
140	2003	35	2	387,298	Somali Civil War	
141	2004	34	2	223,607	Lord's Resistance Army insurgency	
142	1991	7	4	38,000	Nagorno-Karabakh War	
143	1991	2	2	32,091	Gulf War	
144	1997	12	3	93,808	Algerian Civil War	
145	1993	5	4	100,903	Bosnian War	
146	1991	1	2	141,333	1991 Iraqi Civil War	
147	1997	12	3	122,474	Sierra Leone Civil War	
148	1999	13	3	300,000	Burundian Civil War	
149	1994	1	2	800,000	Rwandan genocide	
150	1997	2	2	447,214	First Congo War	
151	2001	6	4	3,674,235	Second Congo War	
152	2001	5	2	60,000	Ituri conflict	Part of the Second Congo War
153	2011	20	4	585,423	War on Terror	
154	2011	20	2	53,949	War in Afghanistan (2001-present)	Part of the War on Terror and War in Afghanistan
155	2007	9	4	190,000	Iraq War	Part of the War on Terror
156	2012	18	4	300,000	War in Darfur	
157	2012	17	4	100,000	Kivu Conflict	Part of the Second Congo War
158	2012	17	8	60,165	War in North-West Pakistan	Part of the War on Terror and War in Afghanistan (2001-present)
159	2013	15	2	200,000	Mexican Drug War	
160	2015	12	4	51,567	Boko Haram insurgency	
161	2016	10	4	570,000	Syrian Civil War	
162	2016	4	4	197,500	Iraqi Civil War (2014–2017)	
163	2018	6	3	91,600	Yemeni Civil War	

References

1. Blum, G. The Paradox of Power: The Changing Norms of the Modern Battlefield. *Houst. Law Rev.* **2019**, *56*, 745–787.
2. Campbell, A. Are We Too Rigid in Our Conception of War. Address Delivered as Chief of the Defence Force, at the Australian Strategic Policy Institute Conference, Canberra. 2019. Available online: https://news.defence.gov.au/media/transcripts/australian-strategic-policy-institute-international-conference-war-2025 (accessed on 10 June 2020).
3. Williams, H.L.; Wright, M.; Evans, T. *A Reader in International Relations and Political Theory*; UBC Press: Vancouver, BC, Canada, 1993.
4. Machiavelli, N. The Project Gutenberg EBook of The Prince, by Nicolo Machiavelli. Online Translation by W. K. Marriott. Available online: https://www.gutenberg.org/files/1232/1232-h/1232-h.htm (accessed on 10 June 2020).
5. Grotius, H. *O Direito da Guerra e da Paz*; UNIJUI: Rio Grande do Sul, Brazil, 2007; Volume 2.
6. Hobbes, T. *The Elements of Law: Natural and Politic*; Oxford University Press: Oxford, UK, 2008.
7. Mannies, W.; Laursen, J.C. Denis Diderot on War and Peace: Nature and Morality. *Araucaria* **2014**, *16*, 155–171. [CrossRef]
8. Clauset, A. On the Frequency and Severity of Interstate Wars. In *Lewis Fry Richardson: His Intellectual Legacy and Influence in the Social Sciences*; Springer, Cham, Switzerland, 2020; p. 113.
9. Standley, V.H.; Nuño, F.G.; Sharpe, J.W. Modeling Interstate War Combat Deaths. *Int. J. Model. Optim.* **2020**, *10*, 8–12. [CrossRef]
10. Cederman, L.E. Modeling the Size of Wars: From Billiard Balls to Sandpiles. *Am. Polit. Sci. Rev.* **2003**, *97*, 135–150. [CrossRef]
11. Pinto, C.; Mendes Lopes, A.; Machado, J. A Review of Power Laws in Real Life Phenomena. *Commun. Nonlinear Sci. Numer. Simul.* **2012**, *17*, 3558–3578. [CrossRef]
12. Newman, M.E. Power Laws, Pareto Distributions and Zipf's Law. *Contemp. Phys.* **2005**, *46*, 323–351. [CrossRef]
13. Bak, P.; Tang, C.; Wiesenfeld, K.; others. Self-organized Criticality: An Explanation of 1/f Noise. *Phys. Rev. Lett.* **1987**, *59*, 381–384. [CrossRef] [PubMed]
14. Jensen, H.J. *Self-Organized Criticality: Emergent Complex Behavior in Physical and Biological Systems*; Cambridge University Press, Cambridge, UK, 1998; Volume 10.
15. Milward, A.S. *War, Economy and Society 1939–1945*; University of California Press: Berkeley, CA, USA; Los Angeles, CA, USA, 1980.
16. Deza, M.M.; Deza, E. *Encyclopedia of Distances*; Springer: Berlin, Germany, 2009.
17. Hartigan, J.A. *Clustering Algorithms*; John Wiley & Sons: Hoboken, NJ, USA, 1975.
18. Aggarwal, C.C.; Hinneburg, A.; Keim, D.A. *On the Surprising Behavior of Distance Metrics in High Dimensional Space*; Springer: Berlin, Germany, 2001.
19. Sokal, R.R.; Rohlf, F.J. The Comparison of Dendrograms by Objective Methods. *Taxon* **1962**, 33–40. [CrossRef]
20. Tenreiro Machado, J.; Lopes, A.M.; Galhano, A.M. Multidimensional Scaling Visualization Using Parametric Similarity Indices. *Entropy* **2015**, *17*, 1775–1794. [CrossRef]
21. Machado, J.T.; Lopes, A.M. Fractional Rényi Entropy. *Eur. Phys. J. Plus* **2019**, *134*, 217. [CrossRef]
22. Valério, D.; Trujillo, J.J.; Rivero, M.; Machado, J.T.; Baleanu, D. Fractional Calculus: A Survey of Useful Formulas. *Eur. Phys. J. Spec. Top.* **2013**, *222*, 1827–1846. [CrossRef]
23. Oldham, K.; Spanier, J. *The Fractional Calculus: Theory and Application of Differentiation and Integration to Arbitrary Order*; Academic Press: New York, NY, USA, 1974.
24. Samko, S.; Kilbas, A.; Marichev, O. *Fractional Integrals and Derivatives: Theory and Applications*; Gordon and Breach Science Publishers: Amsterdam, The Netherlands, 1993.
25. Miller, K.; Ross, B. *An Introduction to the Fractional Calculus and Fractional Differential Equations*; John Wiley and Sons: New York, NY, USA, 1993.
26. Kilbas, A.; Srivastava, H.; Trujillo, J. *Theory and Applications of Fractional Differential Equations*; Elsevier: Amsterdam, The Netherlands, 2006; Volume 204: North-Holland Mathematics Studies.
27. Chen, L.; Pan, W.; Wu, R.; Tenreiro Machado, J.; Lopes, A.M. Design and Implementation of Grid Multi-scroll Fractional-order Chaotic Attractors. *Chaos Interdiscip. J. Nonlinear Sci.* **2016**, *26*, 084303. [CrossRef] [PubMed]

28. Tarasov, V. *Fractional Dynamics: Applications of Fractional Calculus to Dynamics of Particles, Fields and Media*; Springer: New York, NY, USA, 2010.
29. Baleanu, D.; Diethelm, K.; Scalas, E.; Trujillo, J.J. *Fractional Calculus: Models and Numerical Methods*; Series on Complexity, Nonlinearity and Chaos; World Scientific Publishing Company: Singapore, 2012.
30. Ionescu, C. *The Human Respiratory System: An Analysis of the Interplay between Anatomy, Structure, Breathing and Fractal Dynamics*; Series in BioEngineering; Springer-Verlag: London, UK, 2013.
31. Machado, J.T.; Lopes, A.M. The Persistence of Memory. *Nonlinear Dyn.* **2015**, *79*, 63–82. [CrossRef]
32. Yang, X.J.; Baleanu, D.; Srivastava, H.M. *Local Fractional Integral Transforms and Their Applications*; Academic Press: Cambridge, MA, USA, 2015.
33. Lopes, A.M.; Machado, J.T. Integer and Fractional-order Entropy Analysis of Earthquake Data Series. *Nonlinear Dyn.* **2016**, *84*, 79–90. [CrossRef]
34. Beliakov, G.; Sola, H.B.; Sánchez, T.C. *A Practical Guide to Averaging Functions*; Springer: Cham, Switzerland, 2016.
35. Xu, D.; Erdogmuns, D. Renyi's Entropy, Divergence and their Nonparametric Estimators. In *Information Theoretic Learning*; Springer: Cham, Switzerland, 2010; pp. 47–102. [CrossRef]
36. Mingst, K.A.; McKibben, H.E.; Arreguín-Toft, I.M. *Essentials of International Relations*, 8th ed.; W. W. Norton & Company: New York, NY, USA, 2018.
37. Töfekçi, Ö. Can War Ever Be Ethical? Perspectives on Just War Theory Additionally, The Humanitarian Intervention Concept. *Atatürk Univ. J. Econ. Adm. Sci.* **2018**, *32*, 1217–1229.
38. List of Wars by Death Toll. Available online: https://en.wikipedia.org/wiki/List_of_wars_by_death_toll (accessed on 4 April 2020).
39. Carr, J.C.; Fright, W.R.; Beatson, R.K. Surface Interpolation with Radial Basis Functions for Medical Imaging. *IEEE Trans. Med. Imaging* **1997**, *16*, 96–107. [CrossRef] [PubMed]
40. Jackson, M.O.; Morelli, M. *The Handbook on the Political Economy of War*; Edward Elgar Pub: Cheltenham, UK, 2011; Chapter The Reasons for Wars: An Updated Survey.
41. Gutmann, M.P. The Origins of the Thirty Years' War. *J. Interdiscip. Hist.* **1988**, *18*, 749–770. [CrossRef]
42. de Morais, M.V. *Hernán Cortez: Civilizador ou Genocida?* Editora Contexto: São Paulo, Brazil, 2011.
43. Talbott, J.E. Soldiers, Psychiatrists, and Combat Trauma. *J. Interdiscip. Hist.* **1997**, *27*, 437–454. [CrossRef]
44. Jones, E. *The European Miracle: Environments, Economies and Geopolitics in the History of Europe and Asia*, 3rd ed.; Cambridge University Press: Cambridge, UK, 2003.
45. Ferguson, R.B. War Is *Not* Part of Human Nature. War ay not be in our nature after all. *Sci. Am.* **2018**, *319*, 76–81. [CrossRef]
46. Taylor, A.J.P. *The Struggle for Mastery in Europe*; Oxford History of Modern Europe; Clarendon Press: Oxford, UK, 1954.
47. Kimbrough, E.O.; M.Sheremeta, R. Theories of Conflict and War. *J. Econ. Behav. Organ.* **2019**, *159*, 384–387. [CrossRef]